Engineering and Technology Journal
Journal homepage: https://etj.uotechnology.edu.iq

Comparative study on the formability of Aluminum 1100 and Brass CuZn37 in SPIF

Marwa K. Qate'a[a]*, Adnan I. Mohammed[a], Muhsin J. Jweeg[b]

[a] Production Engineering and Metallurgy Dept., University of Technology-Iraq, Alsina'a street, 10066 Baghdad, Iraq.
[b] Technical Engineering Dept., Al-Farahidi University, Baghdad-Jadriya Bridge, Iraq.
*Corresponding author Email: pme.20.67@grad.uotechnology.edu.iq

HIGHLIGHTS

- Aluminum 1100 and Brass CuZn37 were formed using the SPIF process
- The formability was compared based on fracture depth, wall angle, and minimum thickness before fracture
- Aluminum 1100 showed higher formability than Brass CuZn37
- Process parameters had a greater effect on the formability of Brass CuZn37 compared to Aluminum 1100
- Brass alloys can achieve formability similar to aluminum alloys under optimal process conditions

ARTICLE INFO

Handling editor: Israa A. Aziz

Keywords:
SPIF process; Aluminum 1100; Brass CuZn37; Formability; Hyperbolic truncated pyramid.

ABSTRACT

Most research on single-point incremental forming (SPIF) has focused on aluminum sheets of various thicknesses and titanium and steel with moderate mechanical resistance and low thicknesses. However, brass alloys, which exhibit moderate resistance comparable to certain aluminum alloys, have yet to receive much attention from researchers. Consequently, the formability of brass alloys requires a more thorough investigation. This study examines two ductile materials: Aluminum 1100 and Brass CuZn37. Both materials were formed under identical conditions into a hyperbolic truncated pyramid with varying wall angles ranging from 20° to 80° using the SPIF process, with dimensions of 150 mm × 150 mm and a thickness of 0.8 mm. A comparison was made based on fracture depth, maximum wall angle, and minimum thickness before fracture to evaluate the formability of brass alloys in relation to aluminum alloys. The results indicate that while Aluminum 1100 exhibits higher formability than Brass CuZn37, the differences in formability between the two materials are relatively small. The fracture depth, maximum wall angle, and minimum thickness before fracture were 37.1 mm, 80.21°, and 0.24 mm for Aluminum 1100, compared to 34.4 mm, 76.81°, and 0.33 mm for Brass CuZn37. Notably, the effect of process parameters on the formability of Brass CuZn37 was significantly greater than their effect on Aluminum 1100.

1. Introduction

Traditional sheet metal forming processes use dies and molds to form the product, and this technique needs more flexibility, it is primarily used for high-volume production [1,2]. Today, industries increasingly adopt innovative sheet metal forming methods to address current manufacturing challenges and create prototypes using flexible and advanced technologies [3]. Among these methods is the Incremental Sheet Forming process (ISF), developed in the 1990s as a flexible forming method suitable for various industries, including aerospace, automotive, and custom product fabrication. This process, called dieless forming, can produce complex three-dimensional components from sheet metal using relatively simple and cost-effective tools. One variant of this process is Single Point Incremental Forming (SPIF), where sheet metal is progressively and locally deformed using a forming tool controlled by a CNC machine. In this process, while the outer edge of the sheet is clamped and held in place using a blank holder to prevent the sheet from bending, a backing plate is used to support the sheet's reverse side [4-7]. The geometry of the part that needed to be formed was initially designed as a surface model using CAD software, and the tool path consists of multiple contours spaced evenly apart from each other [8-10]. Figure 1 shows the main components of the single-point incremental forming and Figure 2 shows the working principle of the single point incremental forming process. Brasses are copper-zinc alloys with a wide range of engineering applications due to their excellent cold formability, good corrosion resistance, and attractive golden appearance. These qualities facilitate the easy production of various items, including automotive radiator cores, heat exchangers, wind instruments, and decorative components.

http://doi.org/10.30684/etj.2024.151769.1784
Received 27 August 2024; Received in revised form 08 October 2024; Accepted 11 October 2024; Available online 25 November 2024
2412-0758/University of Technology-Iraq, Baghdad, Iraq

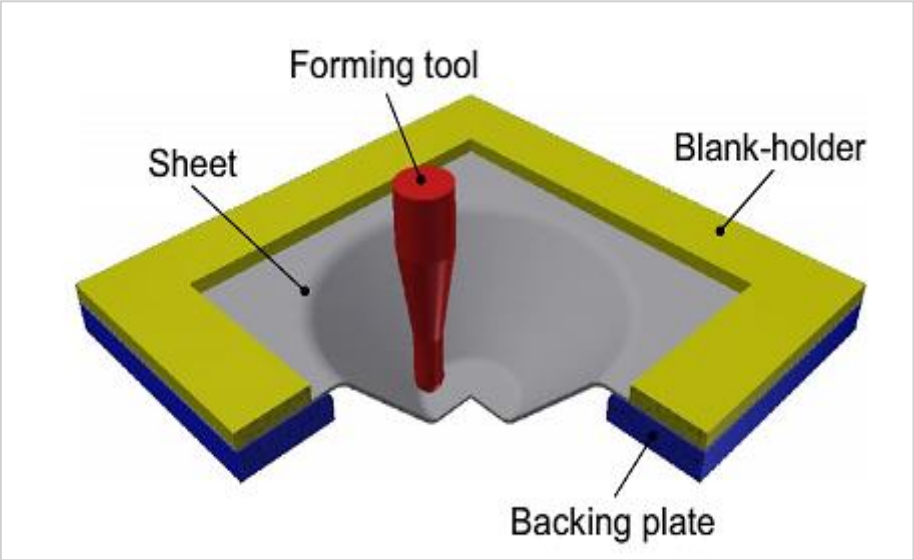

Figure 1: The main components of single point incremental forming are the forming tool, blank holder, backing plate, and sheet metal [5]

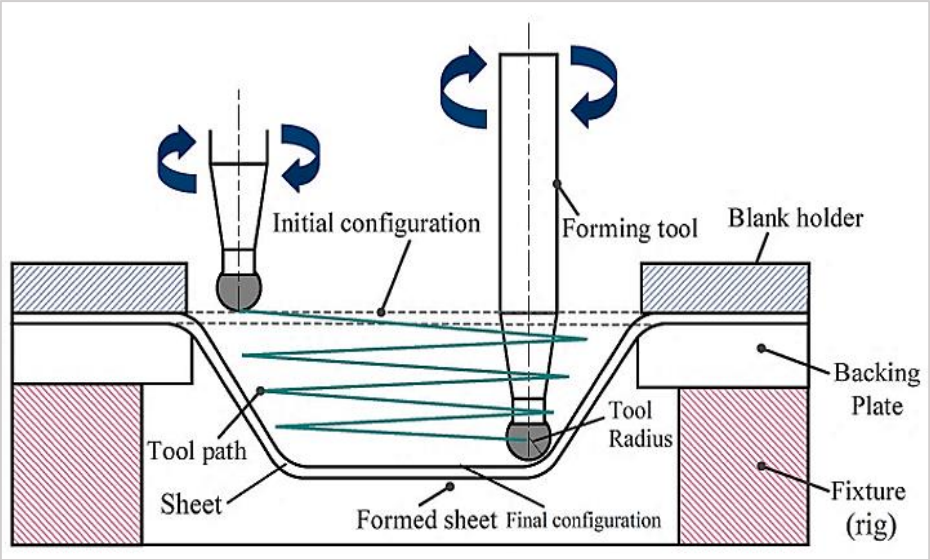

Figure 2: The working principle of SPIF [11]

These characteristics make brass an ideal candidate for ISF technology geared toward low-volume production and customized designs [12]. Despite that, most SPIF research has been conducted on aluminum alloys. The following literature review provides an overview of some main studies that addressed the formability of aluminum alloys in the incremental forming process. Kim and Park [13], examined how different process parameters, such as feed rate, tool type, and size, affect the formability of Al 1050 through experiments and FEM analyses. The results showed that the 10 mm tool diameter shows the best formability, and the formability decreases as the step size increases. Bhattacharya et al. [14], performed an experimental investigation on Al 5052 to evaluate the effects of process variables on the maximum formable angle. The findings reveal that the formability decreases as the tool diameter increases, first increases, then decreases as the step size increases, and feed rate is an insignificant factor in formability. Pandivelan et al. [15], conducted a comprehensive experimental study on SPIF of AA5052 sheets.

A straight groove test was designed to assess the impact of various forming parameters using an L18 orthogonal array. The sum of major and minor strains was measured as an indicator of formability. It is concluded that 900 mm/min is the optimum feed rate value. Abdul Jabar and Younis [16], focused on how depth step, feed rate, and spindle speed affect the formability of Al 1050 H14 in SPIF. The findings revealed that formability decreases as the feed rate and spindle speed increase. Kumar et al. [17], studied the formability of AA2024-O aluminum alloy to examine the effects of various process variables. The results showed that the formability increases directly with an increase in (tool diameter, spindle speed, and sheet thickness), and decreases with an increase in wall angle and step size. Ghazi et al. [18], examined how four process factors, spindle speed, feed rate, tool diameter, and pitch, affect the characteristics of aluminum alloy AA 5010 parts formed by SPIF. It was found that a spindle speed of 1500 RPM, a feed rate of 200 mm/min, a tool diameter of 10 mm, and a step down of 0.4 mm resulted in the lowest maximum thinning and formability.

The present research study focuses on conducting the SPIF process on one of the brass alloy types because these alloys need more attention to form by this process. However, it is widely used in the industry and has excellent cold formability. So

far, the number of research studies on forming brass materials by the SPIF process is limited. Therefore, this work aims to expand the use of the SPIF process on a larger number of materials and not restrict it to specific materials such as aluminum and titanium that were widely used in the previous studies, and to prove the possibility of forming the brass alloys and getting high formability that can match with the formability of some aluminum alloys if they are formed under an optimum condition. Therefore, Aluminum 1100 and Brass CuZn37are used in this work to be formed by SPIF under the same conditions, and the formability of these two materials is compared. This comparison is based on fracture depth, maximum wall angle, and minimum thickness before fracture. Moreover, the degree of the parameter's effect on the formability of each material is also compared.

2. Experimental procedure

The experimental work includes the manufacturing of the forming tools, the manufacturing of the rig, the preparation and testing of the materials used in this work, the identification and creation of the CAD model of the product shape, tool path generation, and finally, the implementation of a set of experiments on a set of specimens using the SPIF technique to investigate the formability of the ductile materials in terms of fracture depth, maximum wall angle (φ_{max}) and minimum thickness before fracture.

2.1 Manufacturing of forming tool

Manufacturing the forming tool requires considering three factors: tool material, tool shape, and tool dimensions. Accordingly, and by using a "CNC turning machine (FANUC Series oi Mate – TC)", three rods of high-speed steel (H.S.S.), each 120 mm in length and 14 mm in diameter were selected to create three hemispherical forming tools with different tool tip diameters (8 mm, 10 mm, 12 mm). Figure 3a depicts the shape and dimensions followed to manufacture the forming tool in this work. Figure 3b illustrates the hemispherical forming tools manufactured and used in this work.

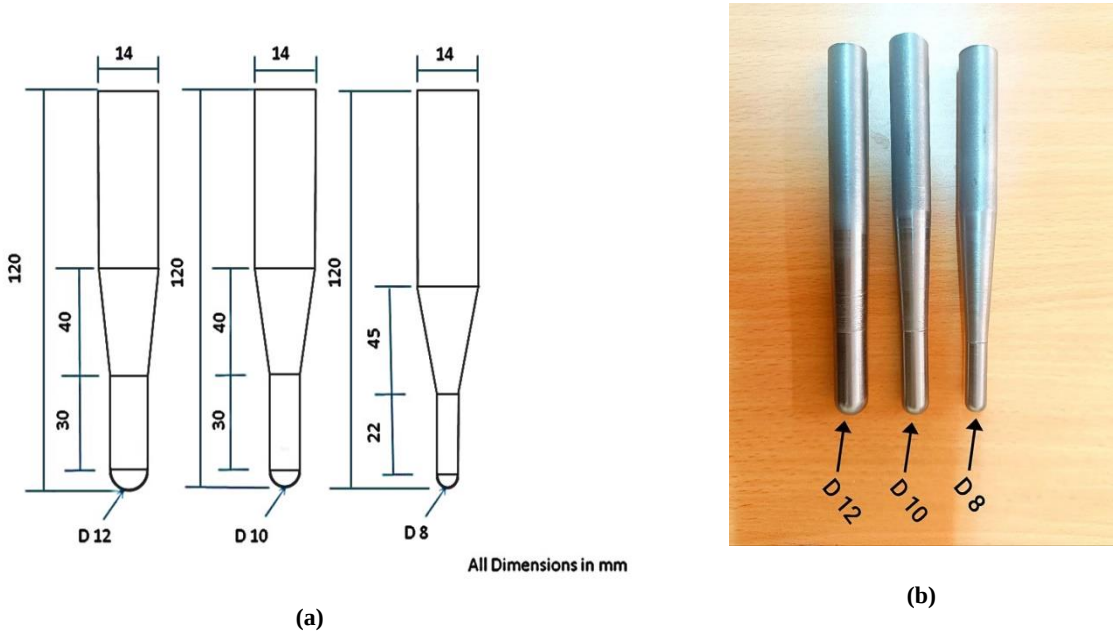

(a) **(b)**

Figure 3: (a) The sketch and dimensions of the hemispherical forming tools, (b) The manufactured tools from the high-speed steel rods

2.2 Manufacturing of rig

The rig needed for performing SPIF was designed and manufactured based on the dimensions provided in Table 1. This rig comprises six main components: base plate, column rod, top plate, backing plate, blank holder, and fasteners. Figure 4 (a, b) shows the rig manufactured in this work.

Table 1: Details of the manufactured rig components

Part	Material	Quantity	Thickness (mm)	Dimensions (mm)
Base plate	Iron	1	8	315 × 215
Column rods	Iron	4	(Dia.) θ 25	120
Top plate	Iron	1	6.5	215 × 315
Backing plate	Iron	1	3	150 × 150
Blank holder	Iron	1	12	215 × 315
Fasteners	Iron	12	—	M 10

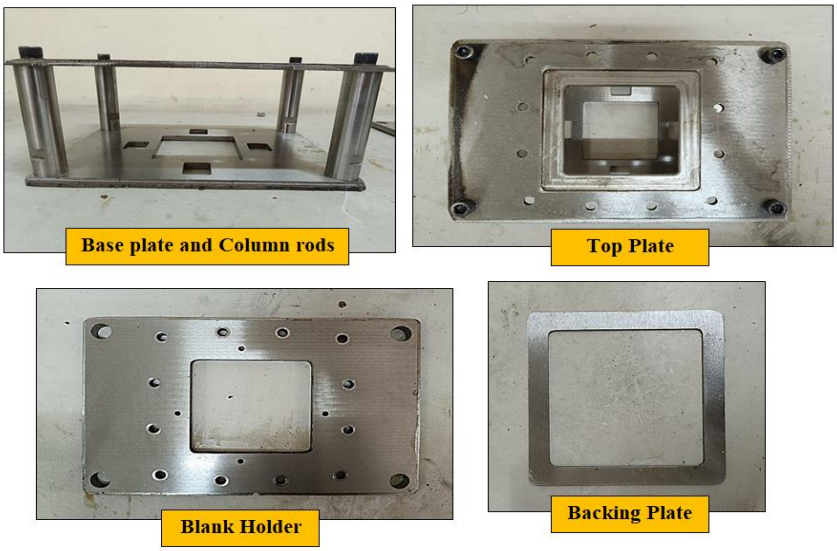

(a)

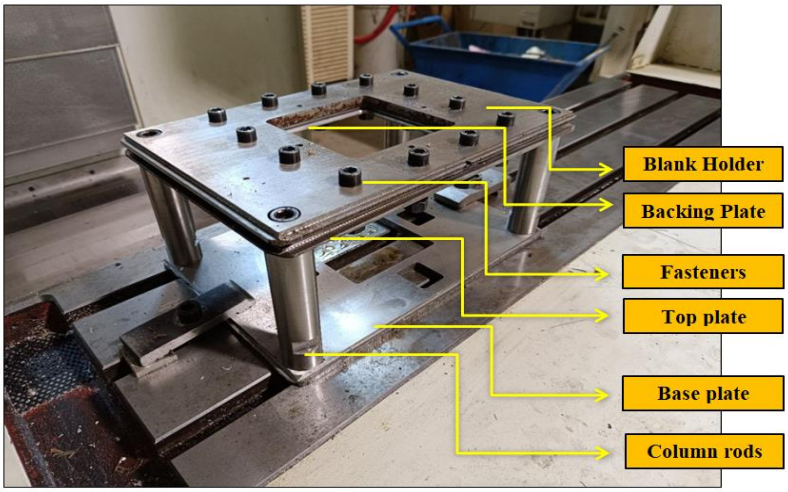

(b)

Figure 4: (a) The five components of the rig (top plate, backing plate, blank holder, base plate, and column rods) that have been manufactured from iron material; (b) The final manufactured and used rig of Single-point incremental forming

2.3 Materials

Two types of ductile materials were used to investigate the formability in the SPIF: Aluminum 1100 and Brass CuZn37, each with dimensions of 150 mm × 150 mm and 0.8 mm sheet thickness. Table 2 illustrates Aluminum 1100 and Brass CuZn37; the chemical composition has been carried out at "the Ministry of Planning / Central Organization for Standardization and Quality Control (COSQC)." Tensile testing was conducted using a "universal testing machine (UTM) model WDW-200e". Tensile specimens were cut from the Aluminum 1100 and Brass CuZn37 sheets at a 90° angle to the rolling direction, according to the E8/E8M ASTM standard depicted in Figure 5. Figure 6 (a, b) displays the standard uniaxial tensile specimens before and after testing, and Table 3 illustrates the mechanical properties of Aluminum and Brass materials.

In industrial applications requiring reduced costs and increased efficiency, Aluminum 1100 would be the ideal choice compared to Brass CuZn37due to its lower cost, high production efficiency in the single-point incremental forming process, and wide availability. While in industrial applications whose basic requirements are durable materials with an attractive appearance and resistance to wear, Brass CuZn37 is the optimal choice compared to Aluminum 1100 because of its superior mechanical properties, high wear and resistance, and aesthetic attractiveness in many unique applications due to its golden color and its ability to develop a pleasing patina over time.

Table 2: Chemical composition of Aluminum 1100 and Brass CuZn37

Al 1100	**Al%**	**Cu%**	**Fe%**	**Si%**	**Mn%**	**Zn%**	**Residual**
	99.3	0.0469	0.371	0.130	0.0340	0.0097	0.0739 (max.)
CuZn37	**Cu%**	**Pb%**	**Fe%**	**Al%**	**Sn%**	**Ni%**	**Zn%**
	63.4	0.0078	0.0229	< 0.0001	0.0525	0.006	36.4

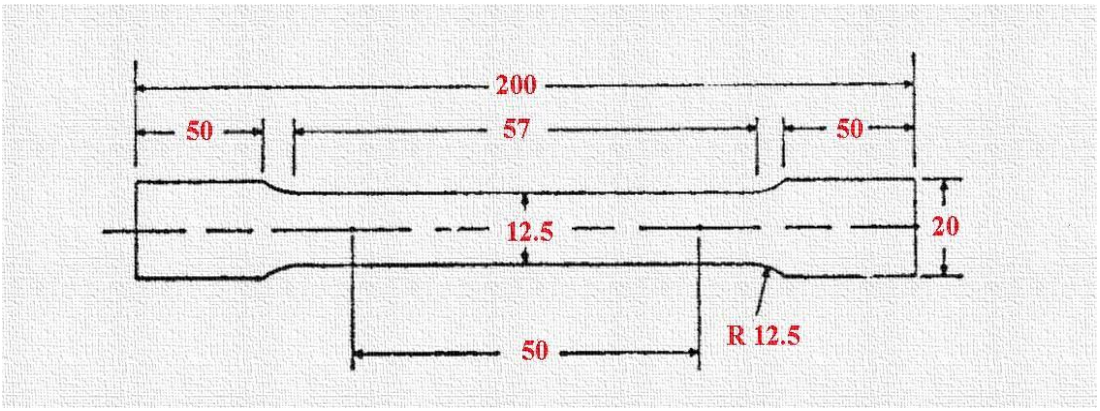

Figure 5: The E8/E8M ASTM tensile test specimen

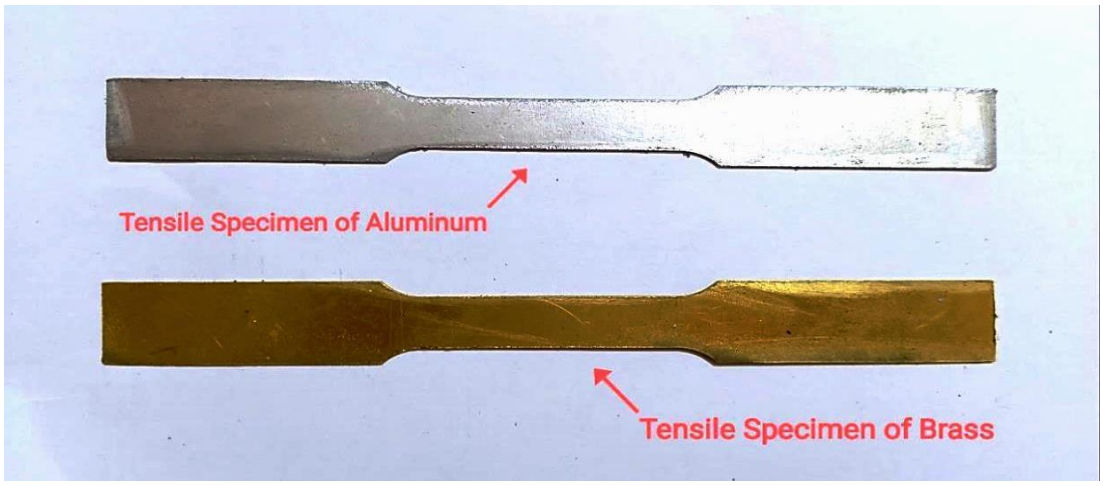

(a)

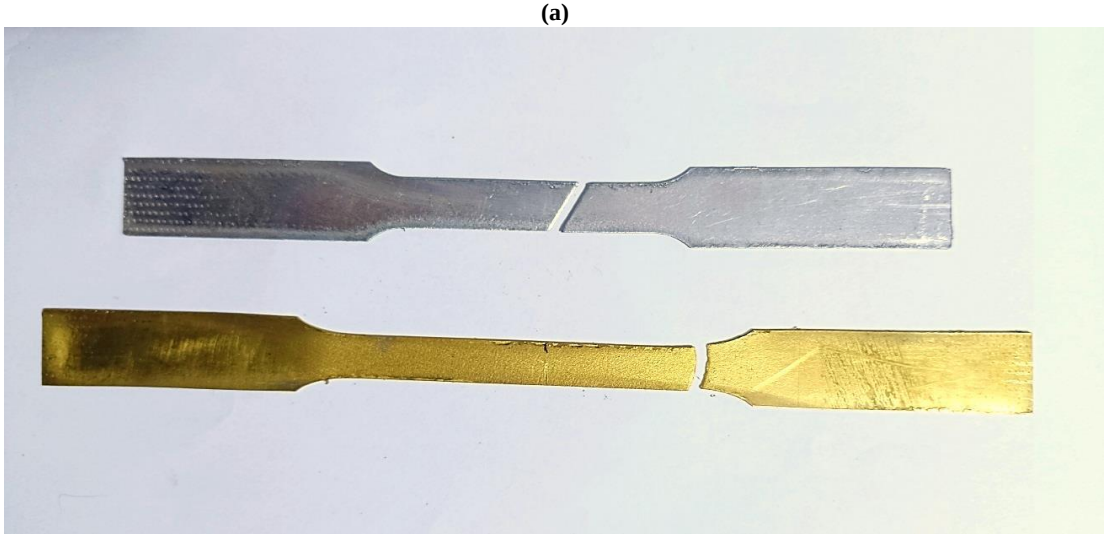

(b)

Figure 6: The standard uniaxial tensile specimens (a) before testing, (b) after testing

Table 3: Mechanical properties of Al 1100 and Brass CuZn37

	Yield stress (MPa)	Tensile strength (MPa)	Modulus of elasticity (GPa)	Density (g/cm^3)	Poisson's ratio
Al 1100	152	187	70	2.71	0.33
CuZn37	254	503	97	8.45	0.34

2.4 CAD model and tool path generation

A hyperbolic truncated pyramid with varying wall angles from 20° to 80° was selected and designed according to the shape sketch, as shown in Figure 7a. The CAD model was designed using Solidworks software, as shown in Figure 7b, to be used later to generate the tool path. The (z-level) tool path was generated using HSMWORKs software to form this product shape, as shown in Figure 8.

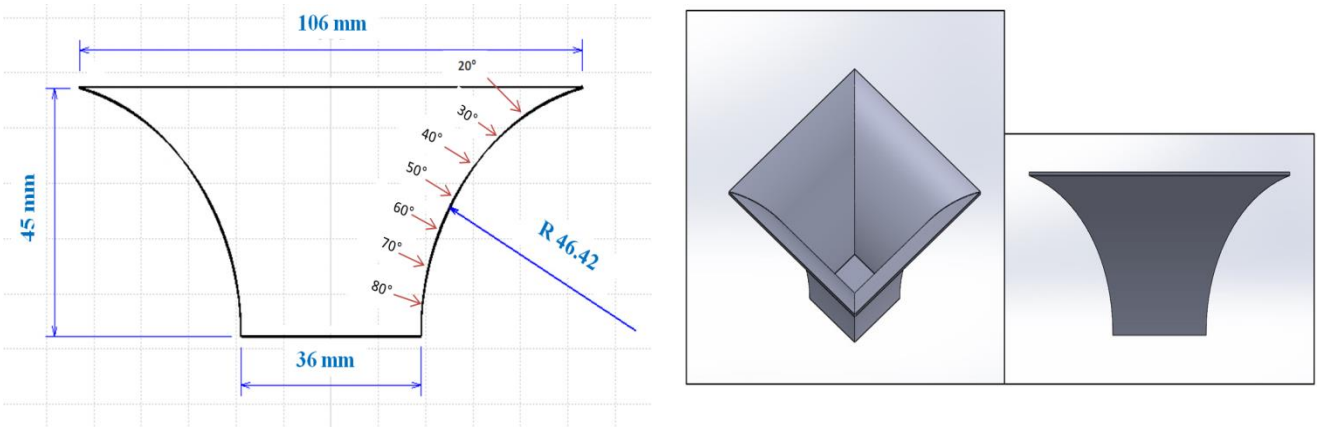

Figure 7: The hyperbolic truncated pyramid with varying wall angles (20°-80°) used in this work (a) The shape sketch with the dimensions, (b) The CAD model created using SolidWorks software

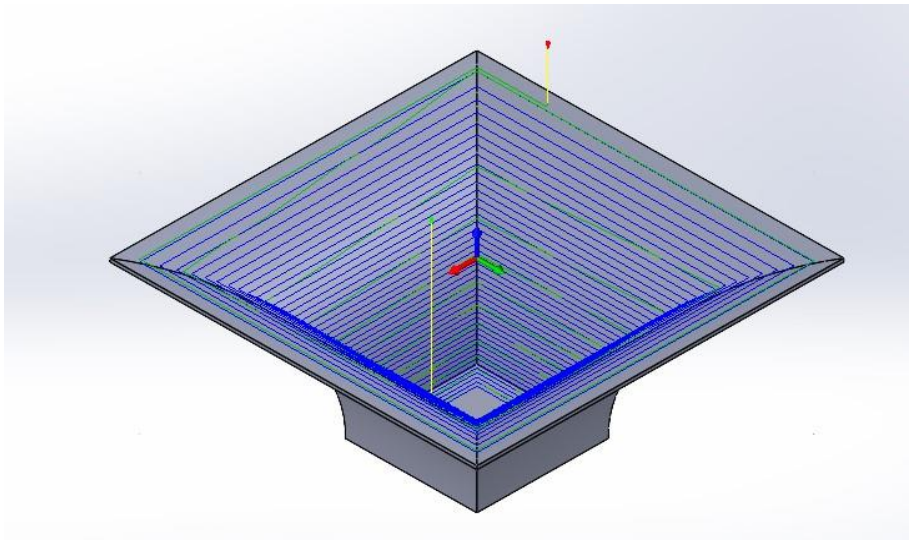

Figure 8: Z-level tool path generated using HSMWORKs software

There are many applications for the hyperbolic truncated pyramid with varying wall angles in different manufacturing industries, especially those requiring complicated and nonlinear geometries. One of these industries is the automotive industry, which can be used in aesthetic components like body panels, engine covers, or trim parts that require a distinctive, stylish look. This geometry can also be used in the aerospace industry due to the varying wall angles that made it reduce drag and improve airflow around the airplane's components. Other applications for this geometry are in the energy field, which is helpful for fluid flow components, like heat exchangers, where gradual transitions in cross-section help reduce turbulence and enhance heat transfer. The flexibility of SPIF makes it feasible to create hyperbolic truncated pyramids with varying wall angles, which are otherwise difficult to achieve through traditional methods that require significant energy costs and very high investment in equipment and dedicated tools, which are complex in design and thus expensive. The design of tooling (die and punch) for complicated shapes is difficult and costly [19].

2.5 Key process parameters

Four input process parameters with three levels each have been chosen for Aluminum 1100 and Brass CuZn37 materials. These parameters include feed rate, tool rotation speed, diameter, and step size. PENNZOIL (SAE 5W-30) is used as a lubricant. Table 4 lists the key process input parameters and their levels and values.

Table 4: Key process input parameters with their levels

Parameter	Unit	Level 1	Level 2	Level 3
Feed rate (*f*)	mm/min	800	1200	1600
Tool rotation speed (ω)	rpm	700	1500	2300
Tool diameter (D)	mm	8	10	12
Step Size (z)	mm	0.3	0.7	1.1

The method that followed to conduct the experiments in this work is based on dividing the experiments of each material into four groups (A, B, C, and D). Each group was divided into three experiments to test three levels (low, moderate, and high) of a specific input parameter that affects the formability (where group A used to test the feed rate, group B to test the tool

rotation speed, group C to test the tool diameter, and group D to test the step size) with keeping the other parameters constant at their moderate level. This method is followed to reach the best level of the tested parameter in each group and use this best level in the rest of the groups. This procedure optimizes the SPIF process and reaches the best parameters that lead to the high formability of aluminum and brass materials. Table 5 illustrates the design of experiments to form the aluminum and brass materials.

Table 5: Design of experiments to form the Al 1100 and Brass CuZn37 materials

			Group A		
Exp. No.	**Feed rate**	**Tool rotation speed**	**Tool diameter**	**Step size**	**Sheet thickness**
GA-1	800				
GA-2	1200	1500	10	0.7	0.8
GA-3	1600				
			Group B		
Exp. No.	**Feed rate**	**Tool rotation speed**	**Tool diameter**	**Step size**	**Sheet thickness**
GB-1	Best Level	700	10	0.7	0.8
GB-2		1500			
GB-3		2300			
			Group C		
Exp. No.	**Feed rate**	**Tool rotation speed**	**Tool diameter**	**Step size**	**Sheet thickness**
GC-1	Best Level	Best Level	8	0.7	0.8
GC-2			10		
GC-3			12		
			Group D		
Exp. No.	**Feed rate**	**Tool rotation speed**	**Tool diameter**	**Step size**	**Sheet thickness**
GD-1	Best Level	Best Level	Best Level	0.3	0.8
GD-2				0.7	
GD-3				1.1	

2.6 Measurement of output responses

Three output responses were measured and considered indicators of the formability of ductile materials in SPIF. These responses are fracture depth, maximum wall angle at which the fracture occurred, and thickness distribution along the wall of the formed part (minimum thickness before fracture). Fracture depth is directly measured from the CNC screen controller when the fracture occurs; the maximum wall angle was measured by returning to the CAD drawing using Solidworks software and checking what the measuring of wall angle at this depth of fracture, while the thickness distribution was measured by using a point micrometer with an accuracy of 0.01 mm in a cut-out section from the formed part by using any cutting device, as shown in Figure 9 (a, b).

(a) **(b)**

Figure 9: (a) cutting out a section from the formed part, (b) Measurement of the thickness distribution along the wall of the formed part using point micrometer

3. Results and discussion

Single point incremental forming process formed twelve sheets of aluminum 1100 and twelve sheets of Brass CuZn37. As previously mentioned, these twelve experiments are divided into four groups (A, B, C, and D), as shown in Table 5. Each group studied the effect of a specific parameter on the formability as follows: Group A studied the impact of feed rate with three levels (800, 1200, and 1600) mm/min, while the other parameters kept constant at their moderate level. Group B studied the effect of tool rotation speed with three levels (700, 1500, and 2300) rpm while keeping the feed rate constant at its best

level and the other parameters constant at their moderate level. Group C studied the effect of tool diameter with three levels (8, 10, and 12) mm while keeping the feed rate and tool rotation speed constant at their best level and the step size constant at their moderate level. Group D studied the effect of step size with three levels (0.3, 0.7, and 1.1) mm while keeping the other parameters constant at their best level. During this and after conducting the experiments of each group, the fracture depth, maximum wall angle, and minimum thickness before fracture are measured to find the best level of this tested parameter.

3.1 Aluminum 1100 experiments

Regarding Al 1100, the results of these groups' experiments were as follows: Experiments of Group A showed that the best value of feed rate is 800 mm/min; Experiments of Group B showed that the best value of tool rotation speed is 2300 rpm; Experiments of Group C showed that the best value of tool diameter is 10 mm; and Experiments of Group D showed that the best value of step size is 0.7 mm. Figure 10 (a- d) shows the experimental specimens with their fracture zones of these groups; the fracture zone is where the material breaks due to excessive strain, damage, or thinning. It marks the point where the formability of the material is exceeded. The material can undergo more deformation when formability is higher before reaching the fracture zone. On the other hand, lower formability leads to earlier failure, typically occurring in localized regions where strain is concentrated, or thinning is most severe; generally, in the previously mentioned Figure, it is observed that the fracture zones occur at a fracture depth ranging between (28 mm and 37.1 mm). For all these specimens of Al 1100, the fracture depths were measured directly from the CNC machine, and according to these fracture depths, the maximum wall angles were measured, as shown in Figure 11 (a-d), which is the steepest angle between the formed surface and the sheet's initial plane. It directly impacts formability since the material is subjected to higher in-plane tensile stresses as the wall angle increases, resulting in more significant strain. Larger wall angles bring the material closer to its formability limits, causing more thinning and increasing the risk of fractures. Then, the thickness distribution along the cutting parts was measured; it describes how the sheet metal's thickness changes during deformation.

As the material is incrementally formed, it typically thins out. This thinning is controlled by the sine law in sheet metal forming, which links the decrease in thickness to the forming angle. As the wall angle increases, the thinning effect becomes more noticeable. A more even thickness distribution across the part indicates better formability, showing that the material is deforming without excessive localized thinning that could cause early failure. In contrast, uneven thickness distribution can lead to early failure and diminish the material's formability. Figure 12 (a-d) shows the plot diagrams of the thickness distribution of Al 1100 specimens. The final results of the measurements of fracture depth, maximum wall angle, and minimum thickness before fractures for Al 1100 have been illustrated in Table 6. The relationship between the fracture zone, wall angle, thickness distribution, and formability is that a larger wall angle leads to increased material thinning and pushes the material closer to its fracture limit, making the thinning more severe and raising the chances of a fracture zone forming. Therefore, formability improves when wall angles are optimized, and thickness distribution is more uniform, reducing strain concentration and preventing early fracture initiation.

From all the previous results, the effect of the parameters (feed rate, tool rotation speed, tool diameter, and step size) on the formability of Al 1100 is summarized as follows: Increasing the feed rate from 800 to 1200 mm/min leads to a constant formability in terms of fracture depth and maximum wall angle, but at the same time, there is very little increase in the minimum thickness before fracturing by 0.01 mm. while increasing the feed rate from 1200 to 1600 mm/min leads to a high decrease in formability in terms of fracture depth and maximum wall angle by 9.1 mm and 11.68°, respectively, with increasing the minimum thickness by 0.12 mm. This agreed with previous literature [15] that showed the optimum feed rate is 900 mm/min, which is located between (800 and 1200 mm/min) in the present work, but it does not agree with [14 and 16]. The previous result showed that the best value of the feed rate is (800 mm/min) which affected the subsequent experiments that tested the effect of tool rotation speed, as increasing the tool rotation speed from 700 to 1500 rpm increases formability in terms of fracture depth and maximum wall angle by 6.3 mm and 8.01°, respectively, and decreases the minimum thickness by 0.06 mm. While increasing the tool rotation speed from 1500 to 2300 rpm produces constant formability regarding fracture depth and maximum wall angle but reduces the minimum thickness before fracturing by 0.04 mm. This agrees with previous literature [17 and 20] but does not agree with [16].

The previous result clarified that the best value of the tool rotation speed is (2300 rpm) which affected the subsequent experiments that tested the effect of tool diameter, as increasing the tool diameter from 8 to 10 mm leads to a little increase in formability in terms of fracture depth and maximum wall angle by 0.7 mm and 0.88°, respectively, while decreasing the minimum thickness by 0.04 mm. While increasing the tool diameter from 10 to 12 mm leads to a decrease in formability in terms of fracture depth and maximum wall angle by 2.1 mm and 2.64°, respectively, with increasing the minimum thickness by 0.04 mm. This agrees with previous literature [13] that showed that the best formability is at a 10 mm tool diameter and with [21] that showed that the formability increases then decreases as the tool diameter increases. Still, it does not agree with [14 and 17]. The previous result clarified that the best value of the tool diameter is (10 mm) which affected the subsequent experiments that tested the effect of step size, as increasing the step size from 0.3 to 0.7 mm leads to a slight increase in formability in terms of fracture depth and maximum wall angle by 0.2 mm and 0.25°, respectively, with a slight decreasing the minimum thickness by 0.01 mm. while increasing the step size from 0.7 to 1.1 mm leads to a little decrease in formability in terms of fracture depth and maximum wall angle by 0.8 mm and 1°, respectively, with increasing the minimum thickness by 0.06 mm. This agrees with the previous literature [14] that showed that the formability increases then decreases with the increase of step size, but it does not agree with [13 and 17]; this previous result showed that the best value of the step size is (0.7 mm).

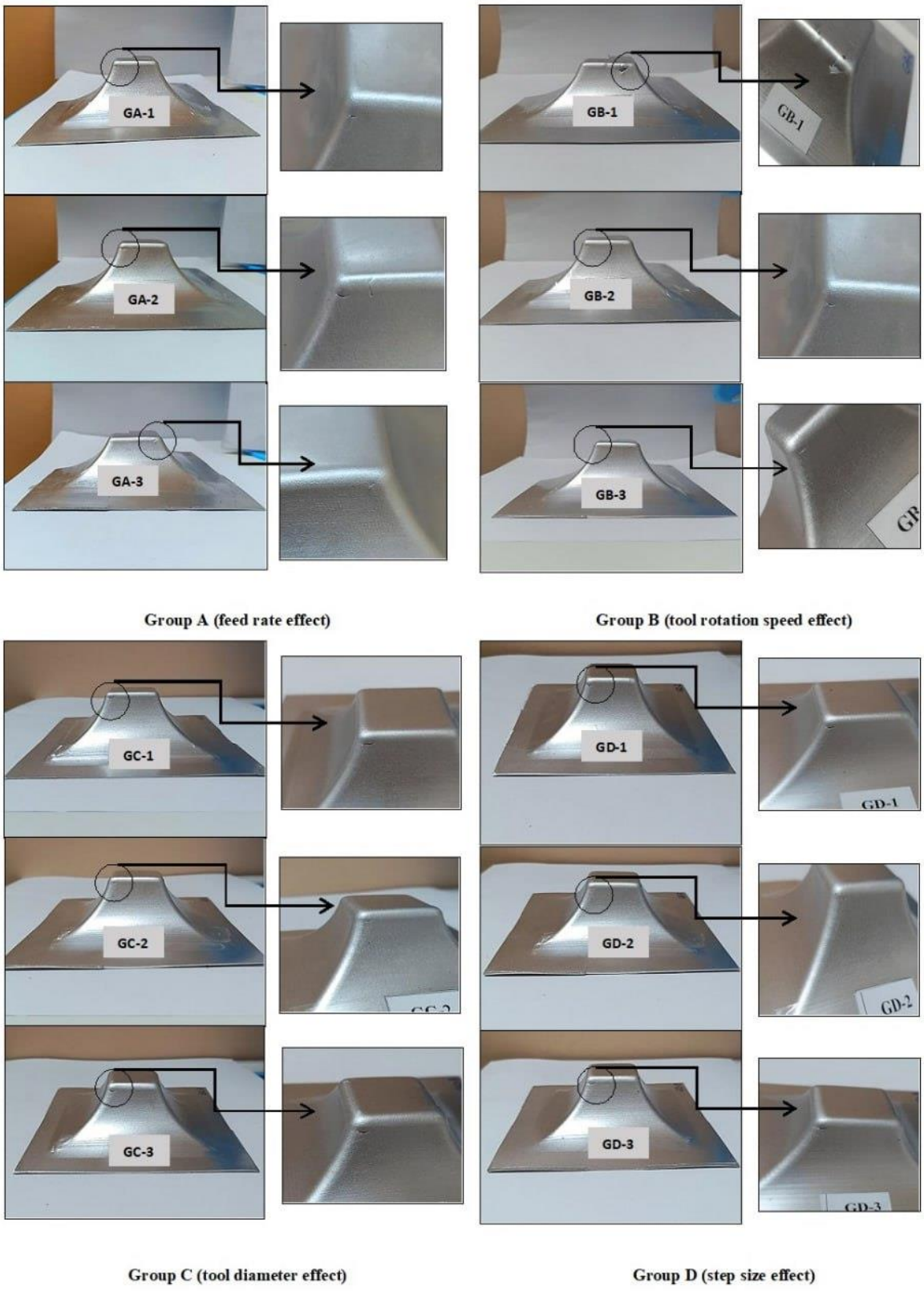

Figure 10: The Aluminum 1100 specimens and their fracture zones that resulted from using the Single-point incremental forming (a) feed rate effect, (b) tool rotation speed effect (c) tool diameter effect, and (d) step size effect

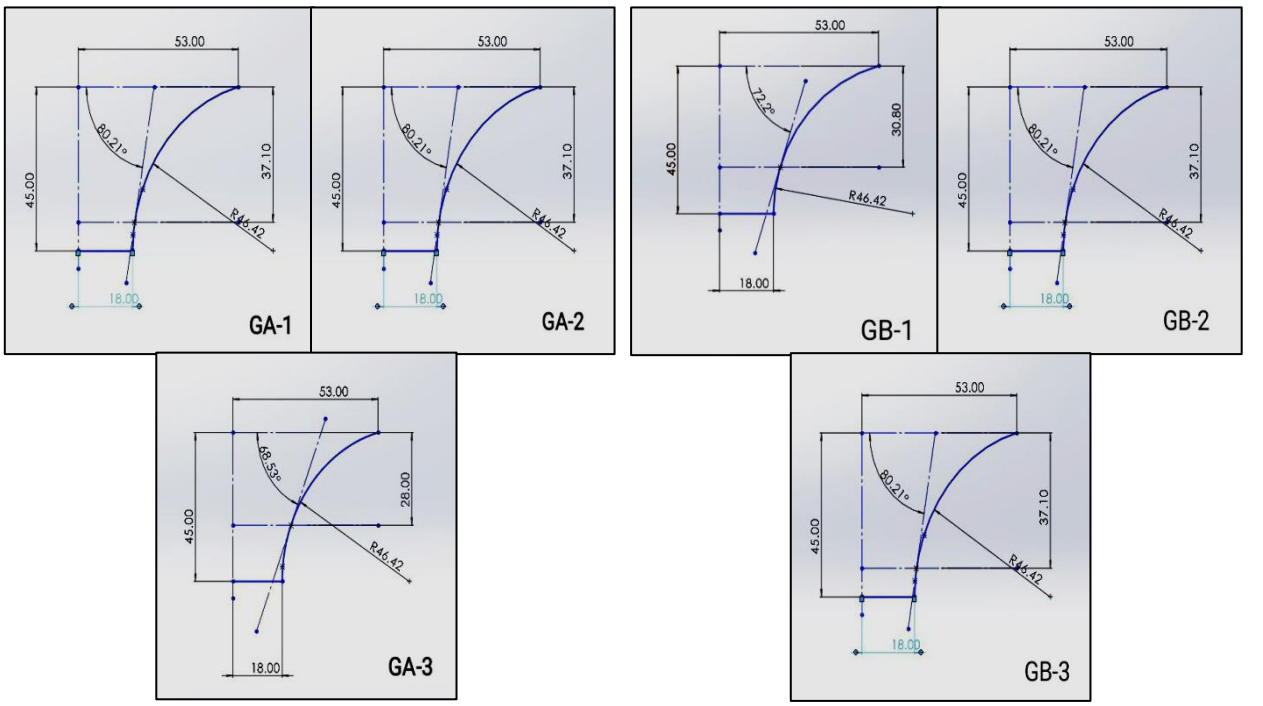

Group A (feed rate effect) **Group B (tool rotation speed effect)**

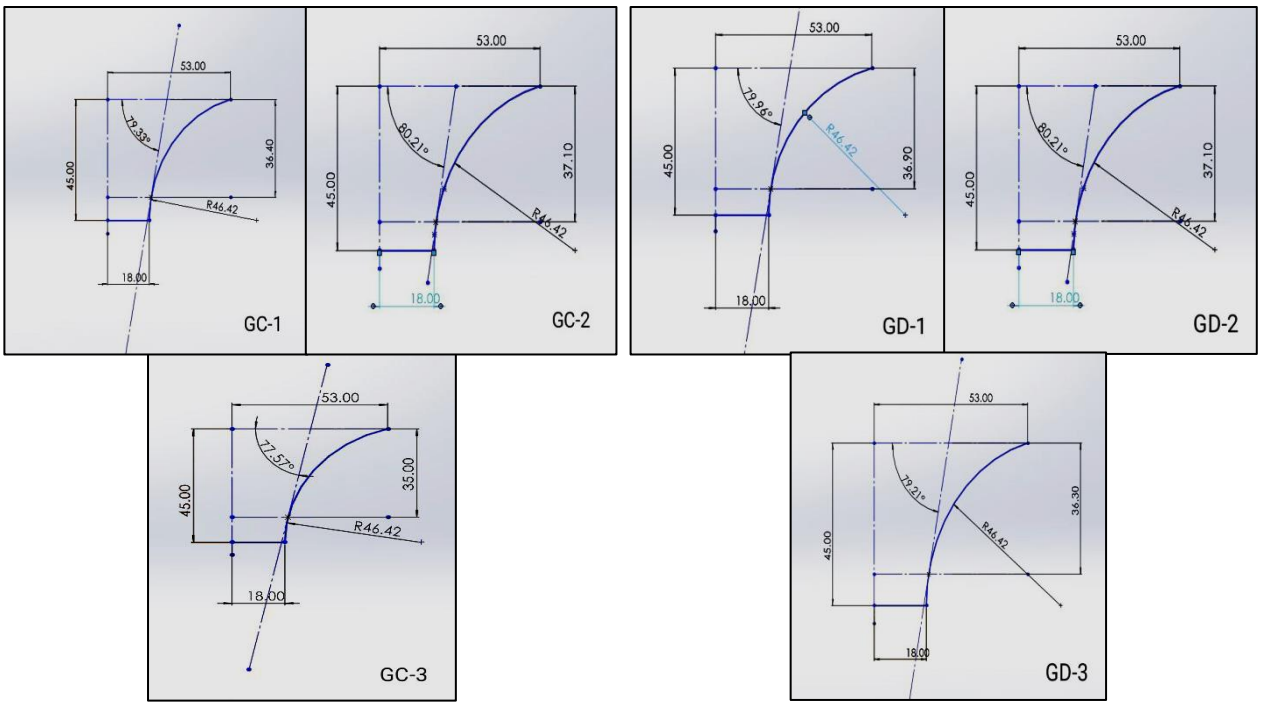

Group C (tool diameter effect) **Group D (step size effect)**

Figure 11: Results of the maximum wall angle measurements of Al 1100 (a) feed rate effect, (b) tool rotation speed effect (c) tool diameter effect, and (d) step size effect

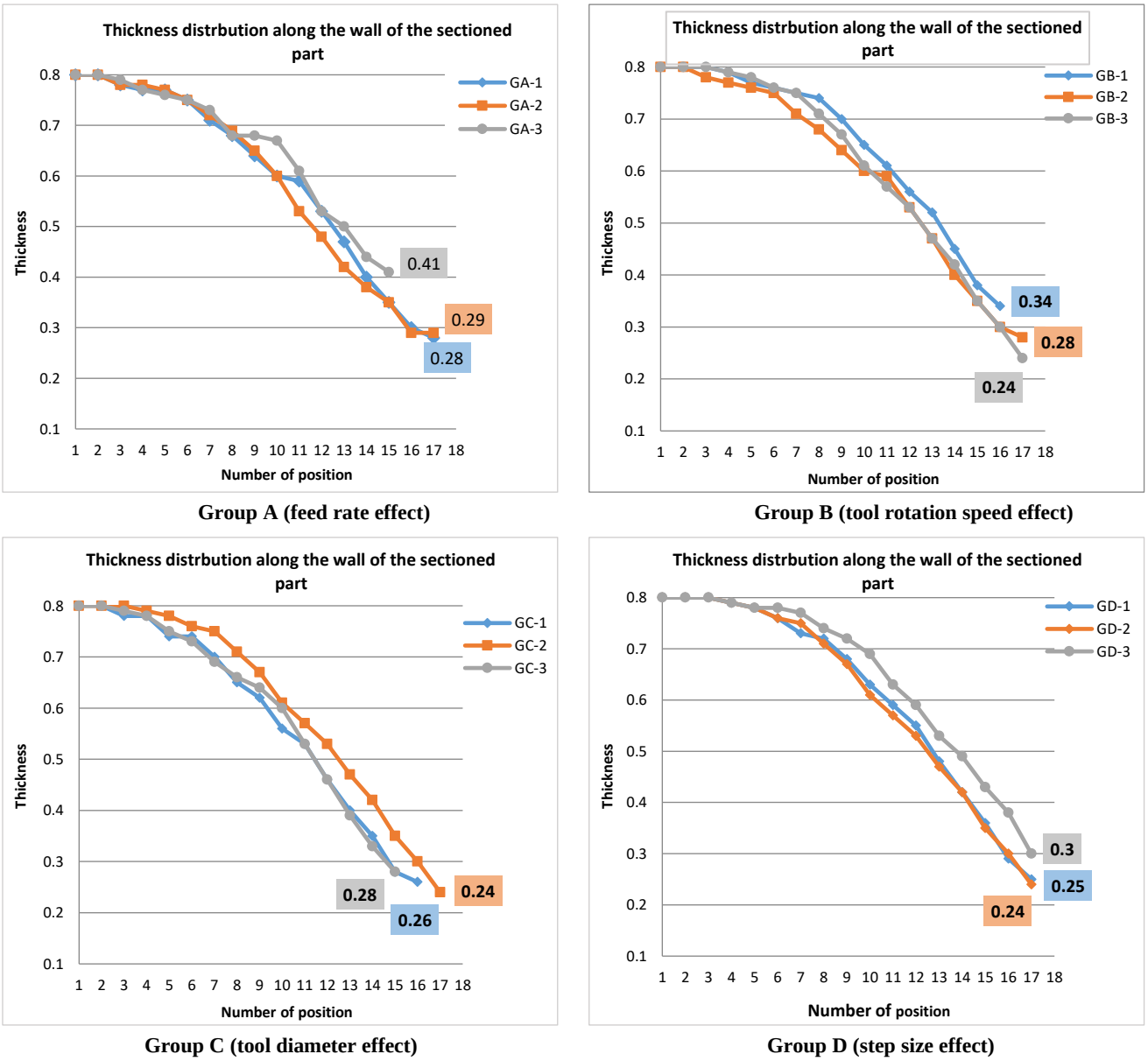

Figure 12: Plot diagram of thickness distribution of Al 1100 (a) feed rate effect, (b) tool rotation speed effect, (c) tool diameter effect, and (d) step size effect

Table 6: Final results of the formability indicators of Al 1100

Level	Parameter	Fracture depth	Maximum wall angle	Minimum thickness
	Feed rate			
Low	800	37.1 mm	80.21°	0.28 mm
Moderate	1200	37.1 mm	80.21°	0.29 mm
High	1600	28 mm	68.53°	0.41 mm
	Tool Speed			
Low	700	30.8 mm	72.2°	0.34 mm
Moderate	1500	37.1 mm	80.21°	0.28 mm
High	2300	37.1 mm	80.21°	0.24 mm
	Tool Diameter			
Low	8	36.4 mm	79.33°	0.26 mm
Moderate	10	37.1 mm	80.21°	0.24 mm
High	12	35 mm	77.57°	0.28 mm
	Step Size			
Low	0.3	36.9 mm	79.96°	0.25 mm
Moderate	0.7	37.1 mm	80.21°	0.24 mm
High	1.1	36.3 mm	79.21°	0.30 mm

3.2 Brass CuZn37 experiments

For Brass CuZn37, the results of the four groups' experiments were as follows: Experiments of Group A showed that the best value of feed rate is 1200 mm/min; Experiments of Group B showed that the best value of tool rotation speed is 1500 rpm; Experiments of Group C showed that the best value of tool diameter is 10 mm; and Experiments of Group D showed that the best value of step size is 0.7 mm. Figure 13 (a-d) shows the experimental specimens and the fracture zones of these groups; from this figure, it is observed that the fracture zones occur at a fracture depth ranging between (16.4 mm and 34.4 mm). For all these specimens of Brass CuZn37, the fracture depths and then the maximum wall angles were measured, as shown in Figure 14 (a-d). Figure 15 (a-d) shows the plot diagrams of the thickness distribution of Brass CuZn37, and the final results of the measurements of fracture depth, maximum wall angle, and minimum thickness before fractures for Brass CuZn37 have been illustrated in Table 7.

Table 7: Final results of formability of Brass CuZn37

Level	Parameter	Fracture depth	Maximum wall angle	Minimum thickness
	Feed rate			
Low	800	34.4 mm	76.81°	0.35 mm
Moderate	1200	34.4 mm	76.81°	0.33 mm
High	1600	33.7 mm	75.92°	0.37 mm
	Tool Speed			
Low	700	30.8 mm	72.2°	0.39 mm
Moderate	1500	34.4 mm	76.81°	0.33 mm
High	2300	16.4 mm	52.13°	0.61 mm
	Tool Diameter			
Low	8	21 mm	58.88°	0.52 mm
Moderate	10	34.4 mm	76.81°	0.33 mm
High	12	19.6 mm	56.84°	0.58 mm
	Step Size			
Low	0.3	25.2 mm	64.76°	0.45 mm
Moderate	0.7	34.4 mm	76.81°	0.33 mm
High	1.1	16.5 mm	52.13°	0.60 mm

The effect of these parameters on the formability of Brass CuZn37 is summarized as follows: Increasing the feed rate from 800 to 1200 mm/min leads to a constant formability in terms of fracture depth and maximum wall angle, but at the same time, there is a slightly decreasing in the minimum thickness before fracture by 0.02 mm. while increasing the feed rate from 1200 to 1600 mm/min leads to a little decrease in formability in terms of fracture depth and maximum wall angle by 0.7 mm and 0.89°, respectively and leads to increasing the minimum thickness before fracture by 0.04 mm. This result showed that the best value of the feed rate is (1200 mm/min) which affected the subsequent experiments that tested the effect of tool rotation speed, as increasing the tool rotation speed from 700 to 1500 rpm increases formability in terms of fracture depth and maximum wall angle by 3.6 mm and 4.61°, respectively and decreases the minimum thickness by 0.06 mm. while increasing the tool rotation speed from 1500 to 2300 rpm leads to a very high decrease in formability in terms of fracture depth and maximum wall angle by 18 mm and 24.68°, respectively, with a high increasing in the minimum thickness before fracture by 0.28 mm. This result clarified that the best value of the tool rotation speed is (1500 rpm) which affected the subsequent experiments that tested the effect of tool diameter, as increasing the tool diameter from 8 to 10 mm leads to a very high increase in formability in terms of fracture depth and maximum wall angle by 13.4 mm and 17.93°, respectively, and decreases the minimum thickness by 0.19 mm. Increasing the tool diameter from 10 to 12 mm leads to a very high decrease in formability in terms of fracture depth and maximum wall angle by 14.8 mm and 19.97°, respectively, with increasing the minimum thickness before fracture by 0.25 mm. This result clarified that the best value of the tool diameter is (10 mm) which affected the subsequent experiments that tested the effect of step size, as increasing the step size from 0.3 to 0.7 mm increases formability in terms of fracture depth and maximum wall angle by 9.2 mm and 12.05°, respectively and decreases the minimum thickness by 0.12 mm. while increasing the step size from 0.7 to 1.1 mm leads to a very high decrease in formability in terms of fracture depth and maximum wall angle by 17.9 mm and 24.68°, respectively, and leads to a high increase in the minimum thickness before fracture by 0.27 mm, this result showed that the best value of the step size is (0.7 mm).

However, the formability of Al 1100 remains higher than that of Brass CuZn37 due to some of the properties of the materials. The first one is that the Brass CuZn37 has less ductility than Al 1100, which makes it more susceptible to cracks and premature fracture under high strain in SPIF. The second is that Al 1100 has higher fracture toughness compared to Brass CuZn37, which enables it to absorb more energy before failure. The third property is that the Brass CuZn37 has a higher work hardening rate than Al 1100, which makes it harden more quickly when strained, and this leads to a decrease in the ability of a material to endure large deformation. In addition, the increase in material hardness makes it brittle as soon as possible and hence increases the chance of fracture risk. The fourth property is related to the fact that the Brass CuZn37 has a lower thermal conductivity compared to Al 1100. This means that the brass does not benefit much from the softening that resulted from the heat generated during the process, and therefore this will lead to less formability. Because of that, the material, in this case, becomes more brittle when it is exposed to high temperatures and localized heating.

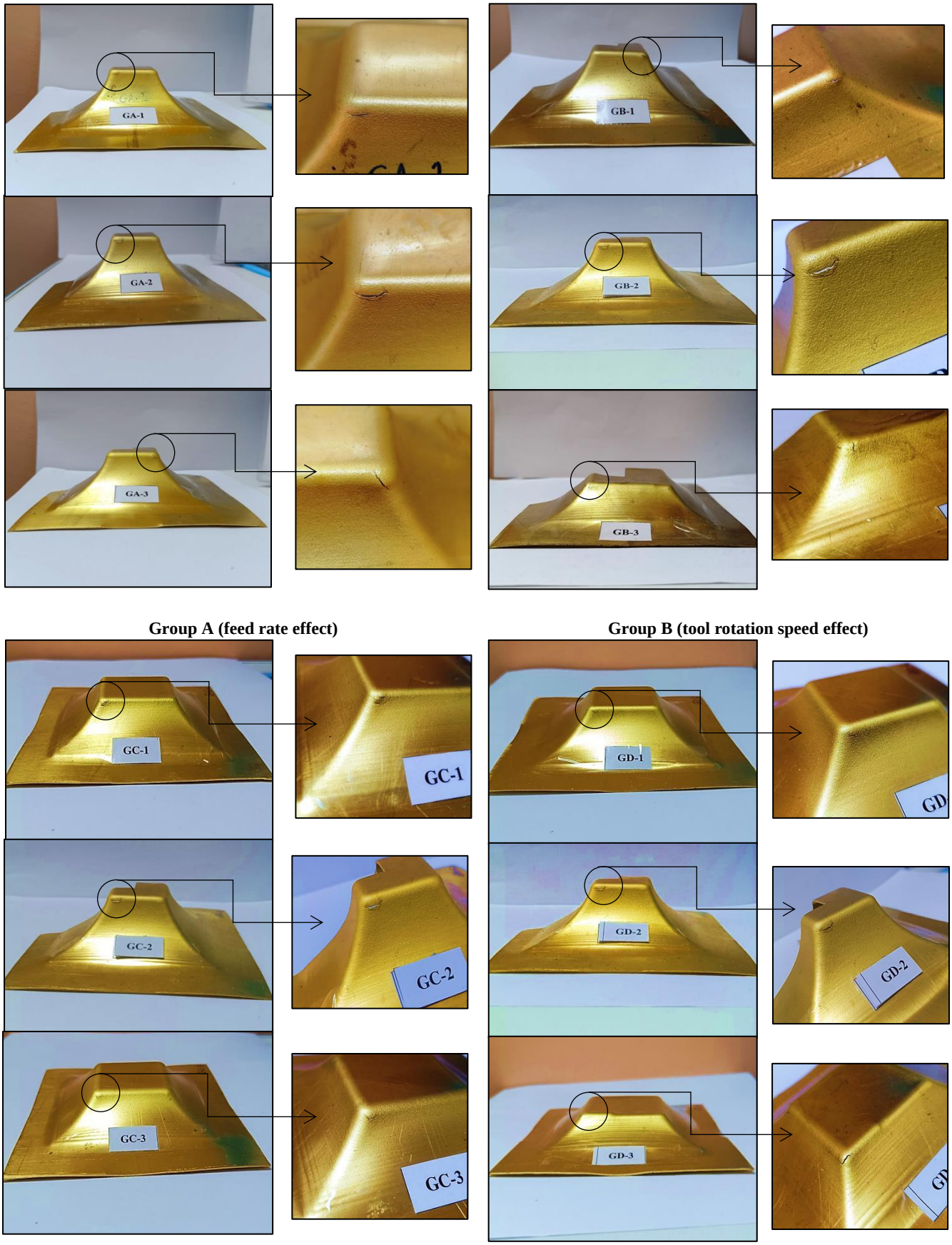

Figure 13: The Brass CuZn37 specimens and their fracture zones that resulted using the single point incremental forming (a) feed rate effect, (b) tool rotation speed effect, (c) tool diameter effect, and (d) step size effect

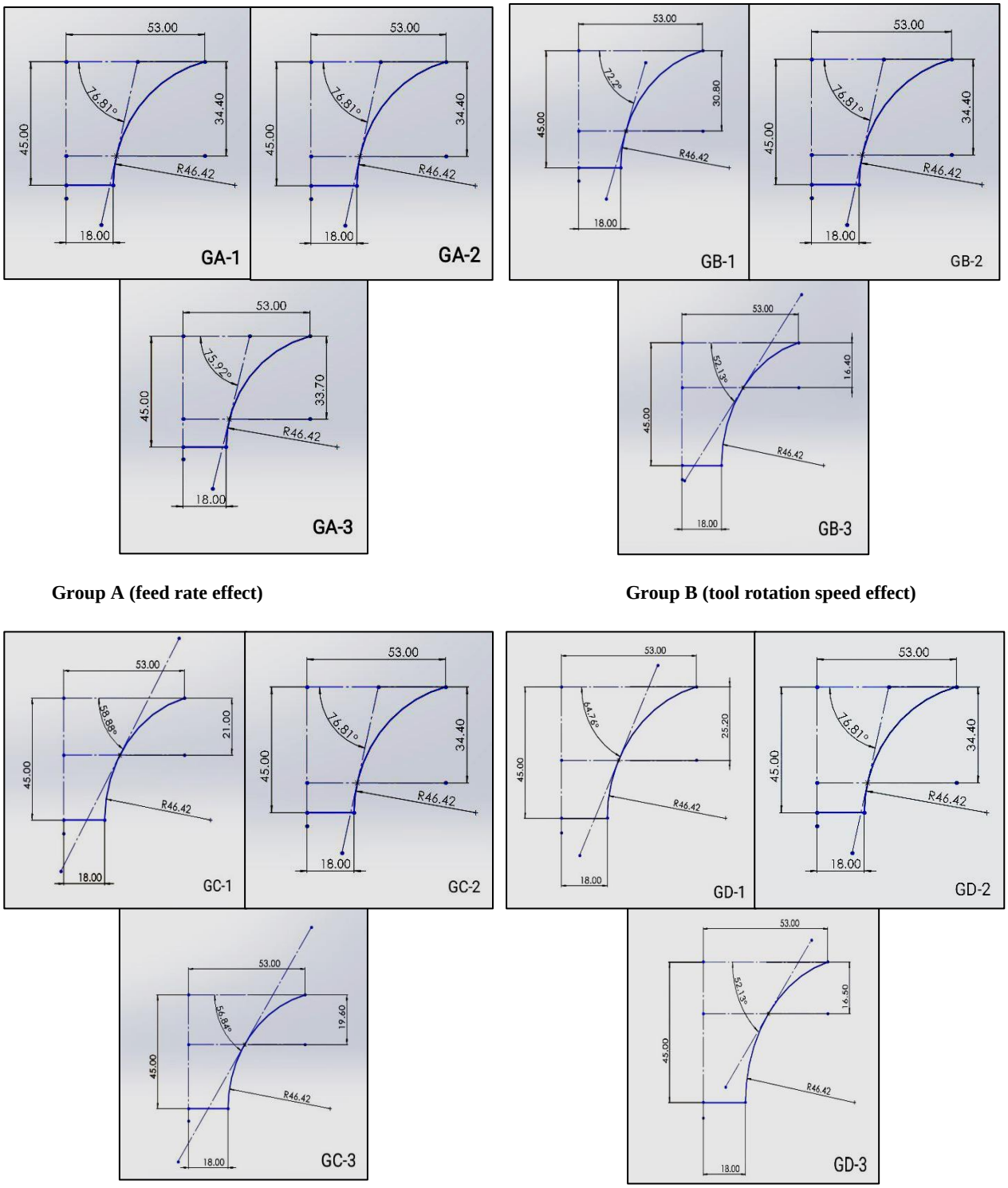

Group A (feed rate effect) **Group B (tool rotation speed effect)**

Group C (tool diameter effect) **Group D (step size effect)**

Figure 14: Results of the maximum wall angle measurements of Brass CuZn37(a) feed rate effect, (b) tool rotation speed effect, (c) tool diameter effect, and (d) step size effect

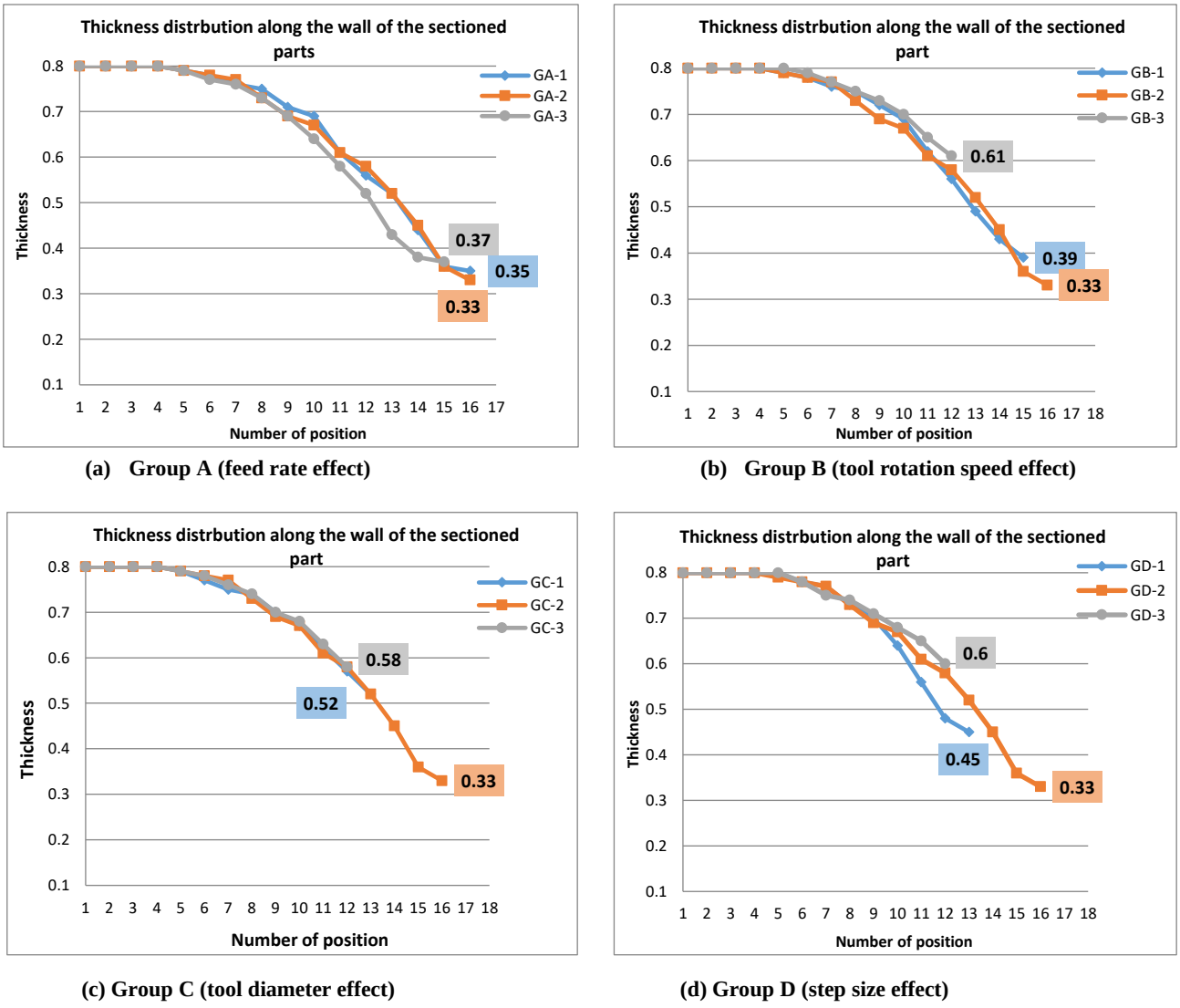

(a) Group A (feed rate effect) **(b) Group B (tool rotation speed effect)**

(c) Group C (tool diameter effect) **(d) Group D (step size effect)**

Figure 15: Plot diagram of thickness distribution of Brass CuZn37 (a) feed rate effect, (b) tool rotation speed effect, (c) tool diameter effect, and (d) step size effect

When comparing the effect of parameters on the formability of Aluminum 1100 and Brass CuZn37 from the previous results of sections (3.1 and 3.2) it is can be summarized these effects as illustrated in Table 8.

Table 8: The summary of the input parameters effect on the formability of Aluminum 1100 and Brass CuZn37

Parameter	Level	Formability of Al 1100	Formability of Brass CuZn37	Degree of parameter effect on formability
Feed rate	Low - Medium	Constant	Constant	—
	Medium - High	Decreasing	Decreasing	Al 1100 >> Brass CuZn37
Tool speed	Low - Medium	Increasing	Increasing	Al 1100 ≈ Brass CuZn37
	Medium - High	Constant	Decreasing	Its effect on brass is very much
Tool diameter	Low - Medium	Increasing	Increasing	Brass CuZn37 >> Al 1100
	Medium - High	Decreasing	Decreasing	Brass CuZn37 >> Al 1100
Step size	Low - Medium	Increasing	Increasing	Brass CuZn37 >> Al 1100
	Medium - High	Decreasing	Decreasing	Brass CuZn37 >> Al 1100

3.3 The physical explanations of parameters effects

It is observed that the physical reasons for the effect of the input parameters on formability in the manner previously described are almost similar in Aluminum 1100 and Brass CuZn37 materials. The impact of the feed rate observed on the formability of both materials is due to the fact that when the value of this parameter is between 800 mm/min and 1200 mm/min, the material will have enough time to adapt to the deformation process, while when the value of this parameter becomes larger than 1200 mm/min, the generated heat will not dissipate because of the high speed of the forming tool movement that hence leads to excessively increasing the frictional heat between the formed sheet and the tool. In addition to that, the larger feed rate values increase the surface roughness and produce the micro cracking that may cause early fracture and decrease the material's ability to be deformed effectively. Moreover, the reasons behind the observed effect of tool rotation speed on formability are that when this parameter is between 700 and 1500 rpm, it leads to improved friction between the sheet

material and the forming tool that generates proper frictional heat, which tends to soften the sheet material to be more ductile and thus enhancing the formability, in contrast when this parameter exceeds 1500 rpm in the brass material, this frictional heat become excessive and leads to thermal degradation of the material properties leads to uneven deformation that results in decreasing of formability.

The physical reason for the relationship that has been noted between the tool diameter and the formability of materials is that when the tool diameter falls between 8 mm and 10 mm, this leads to an increase in the contact zone between the tool and the sheet and hence, allows the strain to disperse across a larger surface. Due to this, the thinning will decrease, and the formability will increase because the deformation becomes more uniform. When the tool diameter exceeds 10 mm, the material flow becomes uneven, and the strain becomes localized, adversely affecting formability. All these behaviors are caused by the extensive increase in the contact zones when the tool diameter is above 10 mm. The observed impact of the step size on the formability is that when the step size falls between 0.3 mm and 0.7 mm, the tool will deform the sheet in more extensive and gradual increments. The strain is distributed across a more extensive area, and this leads to more effective plastic deformation; this is because the tool covers an expanded portion of the sheet with each step. in contrast, when the step size exceeds 0.7 mm, the material displaced with each movement becomes excessive and leads to uneven material flow. The fast deformation also increases the possibility of material thinning, which occurs when the material cannot distribute the strain uniformly, creating weak spots that could cause the fracture to be initiated.

3.4 Statistical analysis

The statistical analysis of the measured outputs (fracture depth and maximum wall angle) for both case of aluminum 1100 and Brass CuZn37 has been performed to enhance the reliability of the results. The confidence interval is a range of values calculated from sample data likely to include the true population parameter (like a population mean or proportion). It helps assess the uncertainty or variability of the sample statistic, this can be calculated using Equations 1 and 2.

$$\text{Confidence Interval (CI)} = \bar{X} \pm \text{MOE} \quad (1)$$

$$\text{Margin of Error (MOE)} = Z \times \left(\frac{s}{\sqrt{n}}\right) \quad (2)$$

where $\bar{X}$: the mean of data, Z: the critical t-value, s: the standard deviation, n: the sample size. And by using excel these parameters have been calculated from the following functions: Mean of data ($\bar{X}$) =AVERAGE(range), Standard deviation (s) =STDEV.S(range), Sample size (n) =COUNT(range), Margin of Error (MOE) =CONFIDENCE.T(1-0.95,standard_dev,size).

The results of the lower and upper confidence interval of the fracture depth and maximum wall angle for Aluminum 1100 and Brass CuZn37 have been illustrated in Table 9.

Table 9: The statistical analysis results of the measured outputs

Statistical Analysis	Aluminum 1100		Brass CuZn37	
	Fracture Depth	**Wall Angle**	**Fracture Depth**	**Wall Angle**
Mean	34.96667	77.49222	25.77778	65.16444
Stdev.	3.3	4.226585	7.681272	10.51883
Count	9	9	9	9
MOE	2.53660455	3.248841	5.90434858	8.08549
Minimum	28	68.53	16.4	52.13
Maximum	37.1	80.21	34.4	76.81
Lower CI (95%)	32.4300621	74.24338	19.8734292	57.07895
Upper CI (95%)	37.5032712	80.74106	31.6821264	73.24993

4. Conclusion

According to the results obtained from this work, the main conclusions can be summarized as the following:

1) Under the same conditions, both ductile materials (Aluminum alloy 1100 and Brass CuZn37 alloy) exhibit good formability in the SPIF technique. Aluminum 1100 has higher formability than Brass CuZn37, but the formability results of both materials are almost similar under the optimum process conditions.
2) The maximum and minimum fracture depths for Al 1100 are 37.1 mm and 28 mm, respectively, from the total product depth of 45 mm, while for Brass CuZn37, they are 34.4 mm and 16.4 mm, respectively.
3) The maximum and minimum wall angles obtained experimentally for Al 1100 are 80.21° and 68.53°, respectively, from the maximum wall angle value of 90°, while for Brass CuZn37; they are 76.81° and 52.13°.
4) The minimum thickness before fracture for Al 1100 specimens ranges between 0.24 mm and 0.41 mm for a thickness of 0.8 mm, while for Brass CuZn37 specimens, it ranges between 0.33 mm and 0.61 mm.
5) The best level of parameters in the case of Aluminum 1100 is as follows: feed rate (800 mm/min), tool rotation speed (2300 rpm), tool diameter (10 mm), and step size (0.7 mm). While the best level of parameters in the case of Brass CuZn37 is as follows: feed rate (1200 mm/min), tool rotation speed (1500 rpm), tool diameter (10 mm), and step size (0.7 mm).
6) According to the results in Table (8), it was concluded that the effect of the parameters on the formability of Al 1100 and Brass CuZn37 is similar regarding their impact on increasing or decreasing the formability of both

materials, but the amount of these effects, especially of (tool rotation speed, tool diameter, and step size) on Brass CuZn37 is much greater than its amount on Al 1100.

7) In summary, it can be concluded that brass alloys can exhibit high formability that can match the formability of aluminum alloys if the process is conducted using optimum parameters, which can be obtained by optimizing the SPIF process.

Author contributions

Conceptualization, M. Qate'a, A. Mohammed and M. Jweeg; data curation, M. Qate'a.; formal analysis, M. Qate'a.; investigation, M. Qate'a; methodology, M. Qate'a, A. Mohammed and M. Jweeg; project administration, M. Qate'a, A. Mohammed and M. Jweeg, resources, M. Qate'a; software, M. Qate'a.; supervision, A. Mohammed and M. Jweeg; validation, M. Qate'a and M. Jweeg.; visualization, M. Qate'a, A. Mohammed and M. Jweeg; writing—original draft preparation, M. Qate'a; writing—review and editing, M. Qate'a. All authors have read and agreed to the published version of the manuscript.

Funding

This research received no specific grant from any funding agency in the public, commercial, or not-for-profit sectors.

Data availability statement

The data that support the findings of this study are available on request from the corresponding author.

Conflicts of interest

The authors declare that there is no conflict of interest.

References

[1] A. K. Jassim, A. S. Hammood, Single Roll Melt Spinning Technique Applied as a Sustainable Forming Process to Produce Very Thin Ribbons of 5052 and 5083 Al-Mg Alloys Directly from Liquid State, Proc. CIRP, 40 (2016) 133 - 137. https://doi.org/10.1016/j.procir.2016.01.079

[2] H. A. Habeeb, M. J. Jweeg, A. A. Khalif, Investigation of the Effect of SPIF Parameters on the Thickness of Al 2024 Alloy, Eng. Technol. J., 41(2023)1627-1637. https://doi.org/10.30684/etj.2023.143718.1604

[3] M. Dwivedy,V. Kalluri, The effect of process parameters on forming forces in single point incremental forming, Procedia, Manuf., 29 (2019)120 -128. https://doi.org/10.1016/j.promfg.2019.02.116

[4] Snehal, V. Parametric investigation on single point incremental forming for difficult to form material. Ph.D. Thesis, Gujarat Technological University, 2019.

[5] D. M. Neto, J. M. Martins, M. C. Oliveira, L. F. Menezes, J. L. Alves, Evaluation of strain and stress states in the single point incremental forming process, Int. J. Adv. Manuf. Technol., 85 (2016) 521-534. https://doi.org/10.1007/s00170-015-7954-9

[6] H. Wei, G. Hussain, X. Shi, B. B. Isidore, M. Alkahtani, M. H. Abidi, Formability of Materials with Small Tools in Incremental Forming, Chin. J. Mech. Eng., 33 (2020) 55. https://doi.org/10.1186/s10033-020-00474-y

[7] L. Chang-Whan, Y. Dong-Yol, Study on the Formability of Magnesium Alloy Sheets in the Incremental Forming Process with External Heating Sources, Int. J. Precis. Eng. Manuf., 21 (2020) 1519-1527. https://doi.org/10.1007/s12541-020-00352-6

[8] S. Gaira, V S. Theja, G. Karthikeyan, Simulation Experimentation of Single Point Incremental Forming of Different Geometries, J. Phys.: Conf. Ser., 1240, 2019, 012007. https://doi.org/10.1088/1742-6596/1240/1/012007

[9] N. T. Nam, N. H. Hiep, N. T. Hung, T. T. Hy, H. H. Han, A Research on The Formability of PVC Sheet in Single Point Incremental Forming (SPIF) Technology, E3S Web Conf., 327, 2021, 05005. https://doi.org/10.1051/e3sconf/202132705005

[10] M. Mohanraj, S. Muhammad, W. Dong, Investigation on Single Point Incremental Forming Process Considering Various Tool Path Definitions, Int. J. Mech. Prod. Eng. Res. Devel., 9 (2019) 511-524. https://doi.org/10.24247/ijmperddec201944

[11] M. Murugesan, D. W. Jung, Formability and Failure Evaluation of AA3003-H18 Sheets in Single-Point Incremental Forming Process through the Design of Experiments, Materials, 14 (2021) 808. https://doi.org/10.3390/ma14040808

[12] S. M. Sudharson, S. Muthupandi, M. Pavithran, T. Parameshwaranpillai, Construction of FLD's on CuZn37(Brass) using Single Point Incremental Forming Technique, Int. J. Innov. Sci. Res. Technol., 3 (2018) 432- 439. https://doi.org/goo.gl/82LiSx

[13] Y. H. Kim, J. J. Park, Effect of process parameters on formability in incremental forming of sheet metal, J. Mater. Proc. Technol., 130 - 131 (2002) 42- 46. https://doi.org/10.1016/S0924-0136(02)00788-4

[14] A. Bhattacharya, K. Maneesh, N. V. Reddy, J. Cao, Formability and surface finish studies in single point incremental forming, J. Manuf. Sci. Eng. Dec., 133 (2011) 061020. https://doi.org/10.1115/1.4005458

[15] P. Chinnaiyan, A. K. Jeevanantham, Multi-objective optimization of single point incremental sheet forming of AA5052 using Taguchi based grey relational analysis coupled with principal component analysis, Int. J. Precis. Eng. Manuf., 15 (2014) 2309-2316. https://doi.org/10.1007/s12541-014-0595-3

[16] A. M. Abdul Jabar, K. M. Younis, Effects of Process Parameters in Incremental Sheet Metal Forming Using Visioplasticity Method, Eng. Technol. J., 34 (2016) 2334-2346., https://doi.org/10.30684/etj.34.12A.15

[17] A. Kumar, V. Gulati, P. Kumar, V. Singh, B. Kumar, H. Singh, Parametric effects on formability of AA2024-O aluminum alloy sheets in single point incremental forming, J. Mate. Res. Technol., 8 (2019) 1461-1469. https://doi.org/10.1016/j.jmrt.2018.11.001

[18] S. K. Ghazi, A. S. Bedan, M. Y. Salloom, Investigating the Impact of Process Parameters on Thinning and Formability in Aluminum Alloy AA 1050 Incremental Sheet Metal Forming, Eng. Technol. J., 41(2023) 1653-1659. https://doi.org/10.30684/etj.2023.143119.1561

[19] Y. Kumar, S. Kumar, Design and Development of Single Point Incremental Sheet Forming Machine, 5th International & 26th All India Manufacturing Technology, Design and Research Conference,(AIMTDR 2014), IIT Guwahati, Assam, India 2014.

[20] I. Alinaghian, H. Ranjbar, M. A. Beheshtizad, Forming Limit Investigation of AA6061 Friction Stir Welded Blank in a Single Point Incremental Forming Process: RSM Approach, Trans. Indian Inst. Met., 70 (2017) 2303-2318. https://doi.org/10.1007/s12666-017-1093-y

[21] K. Maji, G. Kumar, Inverse analysis and multi-objective optimization of single-point incremental forming of AA5083 aluminum alloy sheet, Soft Comput., 24 (2020) 4505- 4521. https://doi.org/10.1007/s00500-019-04211-z